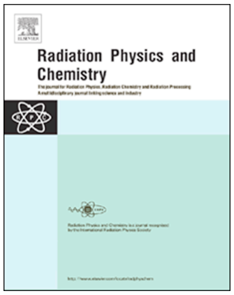

First steps towards online personal dosimetry using computational methods in interventional radiology: Operator's position tracking and simulation input generation

Mahmoud Abdelrahman, Pasquale Lombardo, Filip Vanhavere, Alain Seret, Christophe Phillips, Peter Covens

PII: S0969-806X(19)30952-1

DOI: https://doi.org/10.1016/j.radphyschem.2020.108702

Reference: RPC 108702

To appear in: *Radiation Physics and Chemistry*

Received Date: 31 July 2019

Revised Date: 19 December 2019

Accepted Date: 7 January 2020

Please cite this article as: Abdelrahman, M., Lombardo, P., Vanhavere, F., Seret, A., Phillips, C., Covens, P., First steps towards online personal dosimetry using computational methods in interventional radiology: Operator's position tracking and simulation input generation, *Radiation Physics and Chemistry* (2020), doi: https://doi.org/10.1016/j.radphyschem.2020.108702.

First steps towards online Personal Dosimetry Using Computational Methods in Interventional Radiology: operator's position tracking and simulation input generation

Mahmoud Abdelrahman[1,2], Pasquale Lombardo[1], Filip Vanhavere[1], Alain Seret[2], Christophe Phillips[2], Peter Covens[3]

1 SCK•CEN: the Belgian nuclear research center, Boeretang 200, Mol, 2400, Belgium

2 ULiège: Cyclotron Research Centre, B30, 8 Allée du Six Août, Liège, 4000, Belgium

3 VUB: Vrije Universiteit Brussel – UZ Brussel, Laarbeeklaan 101-103 , 1090 Brussel, Belgium

---

Abstract

Interventional radiologists/cardiologists are repeatedly exposed to low radiation doses which makes them the group of the highest occupational exposure and put them at high risk of stochastic effects. Routine monitoring of staff is usually performed by means of passive dosimeters. However, current personal dosimeters are subject to large uncertainties, especially in non-homogeneous fields, like those found in interventional cardiology (IC). Within the PODIUM (**P**ersonal **O**nline **D**os**I**metry **U**sing computational **M**ethods) research project, a user-friendly tool was developed based on MCNP code to calculate doses to the staff in IC. The application uses both the data of motion tracking system to generate the position of the operator and the data from the Radiation Dose Structure Report (RDSR) from the imaging device to generate time-dependent parameters of the radiation source. The results of the first clinical validation of the system show a difference of about 50% between simulated $H_p(10)$ with MCNP and measured $H_p(10)$ with electronic personal dosimeter worn above the lead apron.

Keywords: Dosimetry, Computations, Interventional Radiology

---

1. Introduction

Interventional radiologists are one of the most occupationally exposed groups to radiation among medical staff working with X-ray [1]. In recent years, the notable advances of medical imaging techniques and the noninvasive nature of such procedures which benefit the patient allowed to increase the number of clinical tasks that can be performed in interventional radiology (IR). As new therapies are developed and the interventions become more advanced, the prolonged duration of X-ray procedures will increase staff radiation exposure [2] and accordingly the daily staff exposure increases their risk of stochastic effects. Some articles discuss a potential correlation between brain and neck cancer incidence among interventional cardiologists and occupational exposure to ionizing radiation [3, 4, 5, 6]. Moreover, an increase in the occurrence of radiation induced eye cataracts among interventional cardiologists has been reported [7, 8, 9].

In such occupational exposure, operators are exposed to non-homogeneous scatter radiation field from the body of the patient while working close by to perform manipulations. The occupational dose is currently determined by means of physical dosimeters. The personal dose equivalent $H_p(10)$ is monitored using physical dosimeters on the trunk, but this sole quantity is often not indicative of the doses delivered to other parts of the body (hands, neck and head). However, monitoring those body parts would require the staff to wear several dosimeters (extremity, eye lens, above/below apron) which is neither practical nor ergonomic. Thus, the non-homogeneity nature of the scatter field in terms of energy and angular distribution increases the uncertainty of the dose estimation using current physical dosimeters [10].

Several commercial Active Personal Dosimeters (APD) that can provide a real-time feedback on the exposure of medical staff in IR are available. The study of Clairand et al. [11] conducted within the ORAMED project shows that some APDs could be used in routine monitoring in IR provided that correction factors are introduced. However, the fundamental problem of monitoring different body parts still exist.

On the other hand, computational dosimetry [12] is becoming an increasingly important tool in assessing radiation exposures. To calculate radiation dose effectively, a computational dosimetry system should comprise two key elements: an accurate computer model of the human body known as anthropomorphic computational phantom, and a numerical technique of radiation transport. Both elements have grown over the past years mainly thanks to the exponential increase and availability of computational power. The computational representation of human body anatomy has evolved: from simple shapes defined with quadratic equations [13], to voxel based representations [14], to the current generation which uses polygonal meshes to represent very realistic anatomy [15]. Similarly, Monte-Carlo simulations of radiation transport continue to get faster [16].

The availability of dose calculation systems that can provide doses to different body parts of staff in IR with better accuracy than current physical dosimeters and in a timely manner can improve dosimetry and increase awareness of radiation risk in among hospital staff.

Badal et al.[17] presented a dose monitoring system based on accurate Monte-Carlo simulations and 3D localization system that can be used to estimate in real-time the average and peak organ doses for both the patient and the staff in interventional fluoroscopy. In this system, a virtual x-ray source graphical interface is used to manually trigger the simulations. The main limitation of the system is the manual operations required to trigger the simulation based on predefined library of beam settings. Also, the system was not tested during clinical procedure.

Within the PODIUM (**P**ersonal **O**nline **D**os**I**metry **U**sing computational **M**ethods) research project, a user-friendly application was developed based on Monte-Carlo simulations to calculate doses to the staff in IC. The application uses both the data of motion tracking system to generate the position of the operator and the data from the Radiation Dose Structure Report (RDSR) from the imaging device to generate time-dependent parameters of the radiation source. The following section describes the methodology used to develop a computational tool for dose calculation and how the system was validated in clinical environment.

2. Materials and Method

The proposed method is making use of a Monte-Carlo code which is provided with different inputs to simulate doses to workers. The two main inputs to our computational dosimetry system are: a) the spatiotemporal parameters of the radiation field, including its energy and angular distribution; b) the relative position and pose of the operator in the radiation field.

2.1. Radiation field parameters

As mentioned previously, interventional cardiologists are exposed to the scatter radiation field from the patient. The scatter radiation is dependent on a number of factors such as primary beam intensity, beam projection angle and patient thickness. Acquiring information about the primary beam and the patient can help reproducing the scatter field computationally in Monte-Carlo simulations. Imaging parameters includes kVp, filtration, collimation and beam projection are used to simulate the primary beam and its scattered field in Monte-Carlo simulations. For that purpose, we use the general-purpose Monte Carlo N-Particle code (MCNP) [18] developed at Los Alamos National Laboratory that can be used for neutron, photon, electron, or coupled neutron/photon/electron transport.

At this stage, the information is obtained from the Radiation Dose Structure Report (RDSR) after each procedure which is a report included in the DICOM (Digital Imaging and Communications in Medicine) dataset that contains various dose-related parameters in a standard format for different modalities. Table(1) shows a sample of a short dose report obtained after a Percutaneous Coronary Intervention (PCI) procedure at CHU-Liège. The report contains enough information that enables the computational tool to generate the primary beam characteristics (spectrum and angulation). Additionally, the measured dose-area product (DAP) value allows to normalize the simulated relative doses (eV/g per particle) to the equivalent absolute dose units. In the future, this information can be accessed online through a communication between the computer that operate the X-ray system and the main computer performing the data acquisition for the simulation.

2.2. Operator motion tracking

The main input to quantify doses to operators is the position and the pose of the operator relative to the X-ray beam and to the patient. Nowadays, depth cameras are able to achieve considerable human body tracking performance in convenient and a low-cost manner. The most famous and widespread depth camera is the Kinect v2 released by Microsoft as a consumer-grade device for human-machine interaction. Kinect v2 is based on

Table 1: Compressed Radiation Dose Report of a Percutaneous Coronary Intervention (PCI) procedure at CHU de Liège

#	**Timestamp**	**kVp**[1]	**mA**[2]	**ms**[3]	**Filter**[4]	**Field** [5]	**t** [6]	**F/s** [7]	**F** [8]	**DAP**[9] μGym^2	**mGy**[1(	**Rot.** [11]	**Tilt** [12]
1	13:17:02	80	284	160.5	0.1Cu	32cm	7s	2F/s	13F	536.5	47.6	0LAO	0CRA
2	13:19:36	125	295	199.6	0.0Cu	32cm	6s	2F/s	11F	1655.2	217	75RAO	0CRA
3	13:20:41	125	295	199.6	0.0Cu	32cm	6s	2F/s	11F	1647.7	216	75RAO	0CRA
4	13:26:03	125	295	199.6	0.0Cu	32cm	5s	2F/s	9F	1347	177	75RAO	0CRA
5	13:26:41	125	295	199.6	0.0Cu	32cm	6s	2F/s	11F	1646.9	216	75RAO	0CRA
6	13:27:08	125	295	199.6	0.0Cu	32cm	6s	2F/s	11F	1647.1	216	75RAO	0CRA
7	13:28:58	125	295	199.6	0.0Cu	32cm	6s	2F/s	11F	1646.7	216	75RAO	0CRA
8	13:29:34	125	295	199.6	0.0Cu	32cm	5s	2F/s	10F	1496.8	196	75RAO	0CRA
9	13:30:46	82	536	160.5	0.0Cu	32cm	6s	2F/s	11F	1090.2	143	27RAO	0CRA

[1] peak kilo-voltage of the x-ray tube that controls the quality of the x-ray beam produced
[2] x-ray tube current in milliampere [3] duration of the x-ray exposure in milliseconds
[4] minimum thickness in mm of the x-ray absorbing material used in the filters [5] field size in diameter
[6] duration of the multi-frame image acquisition [7] number of frames per second of multi-frame image acquisition
[8] total number of frames in a series [9] sum of the area dose product of all images of a series
[10] calculated dose at a reference point
[11] Position of image intensifier about the patient from the right-hand side (RAO) to left-hand side (LAO) direction
[12] position of image intensifier about the patient from the caudal (CAU) to cranial (CRA) direction

time-of-flight principle to reconstruct the third dimension which has considerable higher accuracy over other depth sensing technologies. Processing depth images using a machine learning algorithm allows the Kinect to map the visual data it collects to models representing people of different backgrounds (age, height, gender, body type, clothing,...etc). Microsoft also released a software development kit (SDK) for the Kinect v2 to allow developers to create their applications. In this SDK, a skeleton tracking algorithm based on the method proposed by Shotton et al.[19] is implemented. This approach of skeleton tracking can accurately predict the 3D positions of body joints in real-time with an accuracy within 2-4 cm as found in literature [20, 21, 22].

Our system provides an indoor tracking system for tracking the position and the posture of occupationally exposed workers in cath-labs. The system is constituted by a single Microsoft Kinect v2 TOF camera and by an acquisition software package as shown in figure (1). The tracked skeleton is then used to animate a computational realistic anthropomorphic flexible (RAF) phantom [23] which can be used in either voxel or mesh geometries for different Monte-Carlo tools.

Figure 1: Skeleton tracking during an angiography procedure at UZ-Brussels

2.3. Validation

For validating our system, we performed tests in different IR rooms. In total, we followed 15 procedures of different types: from diagnostic angiogram to Percutaneous Coronary Intervention (PCI) in cath-labs at UZ-VUB and CHU- Liège. Four different main doctors were tracked at different procedures. An accurate analysis of the staff position was performed by evaluating the skeleton tracking performance during irradiation events from the RGB images, the depth images and the skeleton data. Afterwards, and as a first step, we compared simulated $H_p(10)$ with MCNP and measured $H_p(10)$ with electronic personal dosimeter (EPD) Mk2.3 from Thermo Fisher Scientific worn above the lead apron during an angioplasty procedure at CHU-Liège. The procedure was selected where the highest dose to the operator found. After acquiring the tracked skeleton of the main operator during the procedure, these data, together with information from the dose report, were used to generate MCNP input files for the different irradiation events. For that purpose, a user-friendly application was developed to automate the generation of the input files as shown in figure (2). The operational quantity $H_p(10)$ is simulated by tallying energy deposition (MeV/g per particle) in a volume surrounded by a soft-tissue layer of 10 mm thickness and located at the position of the dosimeter obtained from the tracking system. To simplify our model for $H_p(10)$ calculation and for validation purposes only, no phantom was introduced for the operator in the simulations. This could be a reasonable assumption as the study of Ginjaume et. al. [24] shows that the response of most of APDs when they are placed above a lead or lead equivalent garment for x-ray diagnostic qualities to be within 1%–10%.

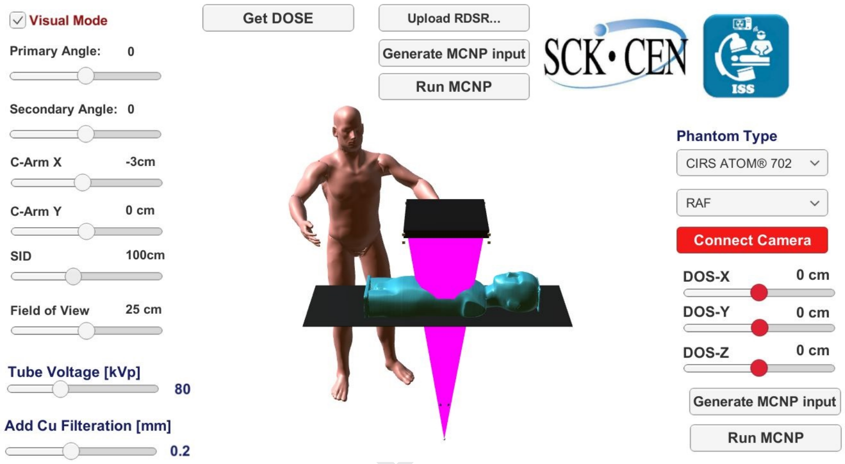
☑ Visual Mode
Primary Angle: 0
Secondary Angle: 0
C-Arm X -3cm
C-Arm Y 0 cm
SID 100cm
Field of View 25 cm
Tube Voltage [kVp] 80
Add Cu Filteration [mm] 0.2
Phantom Type CIRS ATOM® 702
RAF
DOS-X 0 cm
DOS-Y 0 cm
DOS-Z 0 cm

Figure 2: User-friendly application for the generation of MCNP input files with source and geometry configurations in interventional radiology

3. Results and discussion

After the procedure, a short radiation report was obtained from the x-ray system in table(1). During this procedure, the patient received a total reported dose of about 1990 mGy at a reference point which is typically located at 15cm from the iso-center toward the x-ray tube. This quantity is usually derived from the measured Kerma Area Product (KAP) and is used to estimate patient Peak Skin Dose (PSD). In total, 9 irradiation events were reported for the acquisition of images for which three main projections were used: posterior-anterior (PA), 75 degrees to the right-side of the patient (75RAO/0CRA), and 27 degrees to the right-side of the patient (27RAO/0CRA). A simulation MCNP input file for each irradiation event were obtained automatically using the software for different beam settings and irradiation geometry as found in the RDSR.

3.1. Motion tracking of the main operator

As the depth camera was positioned to have a complete view of the operator, the upper part of the main operator's body could be tracked throughout the procedure especially during irradiation events. The tracking was not hindered by the movable ceiling shield because they are transparent enough to the infrared beam from the Kinect. However, poor skeleton poses sometimes occurred due to occlusions either by persons or objects. One solution to this problem is to use multiple cameras; however, this can add to the complexity of the system in such workplace and creates data fusion problem. Figure (3) shows a sample of the 3-D skeleton of the tracked operator as obtained by the tracking system. The 3-D coordinates of the dosimeter location are used in the simulations.

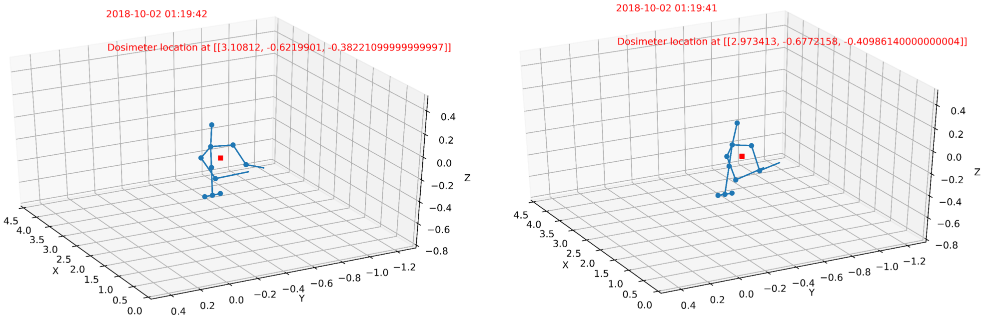

Figure 3: 3-D plot of the tracked skeleton representing the upper body of the first operator during the procedure

The tracked skeleton was recorded and stored in 30 frames per seconds, however, a position every second was used in the simulations to be synchronized with the time intervals in the dose report.

3.2. Dose simulations

An input file for each irradiation event was generated according to the source and the geometry configuration taken from the dose report. The patient was modeled with a BOMAB phantom [25] with a scaled thickness of the thorax of 23 cm to account for a male patient with an average build of 170 cm and 70 kg. Figure(4) shows the particle track output of MCNP for three irradiation events with different beam projections. The total accumulated dose after the procedure, which is obtained by summing up the dose results from each simulation of an irradiation event, is shown in table (2).

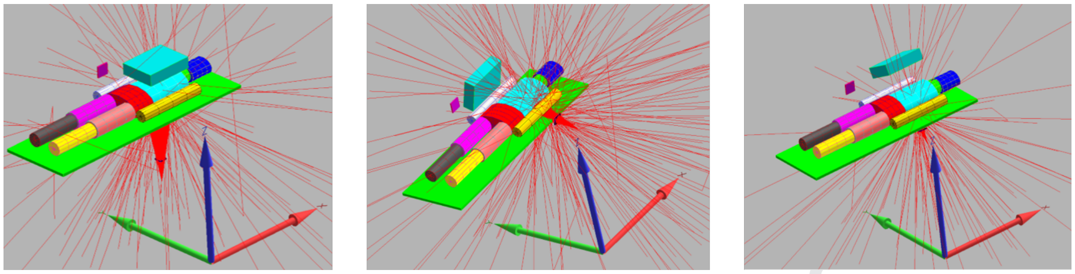

Figure 4: MCNP simulations of the primary and the scattered photons in the procedure for different X-ray beam projections; PA, 75RAO, and 27RAO

Table 2: Total accumulated dose after the procedure

Simulated $H_p(10)$ [μ**Sv**]	**Measured** $H_p(10)$ [μ**Sv**]
38	22

The first operator received a personal dose equivalent, $H_p(10)$, above the lead apron of 22 μSv reported by the EPD. The differences found between the simulations and the measurement can be explained by the uncertainties of the EPD dosimeters. In fact, the study performed by Clairand et al. [11] showed that the EPD Mk2.3 has a variation on the response within 30-40% due to the energy and angular response added to the uncertainty due to the effect of the pulse frequency of the x-ray beam in IR fields.

On the other hand, the main sources of uncertainties in the calculations can be attributed to: the statistical error of Monte-Carlo simulations, the error in the position determination from the tracking system, and the uncertainties in the measured parameters provided by the x-ray devices. The statistical error of Monte-Carlo simulations is usually a trade off for simulation run time. As a first attempt, we decided to keep the error in the simulation below 10%. We could achieve a simulation run time of 30-170 seconds per irradiation event depending on combined effect of beam settings and geometrical configuration. A separate study will follow to optimize the simulation run time at low statistical error within 10% using a smart algorithm that optimize number of particles to be simulated based on beam parameters and the irradiation geometry. The uncertainties related to the measured parameters provided by the x-ray devices can be easily evaluated from the routine calibration according to standards. Finally, the uncertainty associated with the localization of a person by the tracking system can be within 2-4 cm which can impact the error in the dose calculation with additional 5-10%.

4. Conclusion

With this work, we show that simulating worker doses based on tracking systems and flexible phantoms is possible. The proposed computational framework is capable of generating MCNP input files automatically using data from a motion tracking system to generate the position of the operator and the data from RDSR from the imaging device to generate time-dependent parameters of the radiation source for Monte-Carlo simulations to calculate doses to different body parts of the staff in IR/IC. Next step is to use the proposed approach to calculate organ doses and effective dose by using the realistic anthropomorphic flexible (RAF) computational phantom in our Monte-Carlo simulation framework. The optimization of the simulation run time is planned. This method has big advantages in interventional radiology workplaces where the fields are non-homogeneous and doses to staff can be relatively high. This method can also help in ALARA applications and for education and training.

Acknowledgements

PODIUM project is funded by the “CONCERT-European Joint Programme for the Integration of Radiation Protection Research 2014-2018” under grant agreement No. 662287.

References

[1] J. Valentin, Avoidance of radiation injuries from medical interventional procedures, icrp publication 85, Annals of the ICRP 30 (2) (2000) 7–7. doi:10.1016/s0146-6453(01)00004-5.

[2] B. Schueler, T. Vrieze, H. Bjarnason, A. Stanson, An investigation of operator exposure in interventional radiology1, Radiographics : a review publication of the Radiological Society of North America, Inc 26 (2006) 1533–41; discussion 1541. doi:10.1148/rg.265055127.

[3] A. Roguin, J. Goldstein, O. Bar, Brain tumours among interventional cardiologists: A cause for alarm? report of four new cases from two cities and a review of the literature, EuroIntervention : journal of EuroPCR in collaboration with the Working Group on Interventional Cardiology of the European Society of Cardiology 7 (2011) 1081–6. doi:10.4244/EIJV7I9A172.

[4] A. Roguin, J. Goldstein, O. Bar, J. Goldstein, Brain and neck tumors among physicians performing interventional procedures, The American journal of cardiology 111. doi:10.1016/j.amjcard.2012.12.060.

[5] M. Finkelstein, Is brain cancer an occupational disease of cardiologists? can j cardiol, The Canadian journal of cardiology 14 (1998) 1385–8.

[6] E. Picano, E. Vano, The radiation issue in cardiology: the time for action is now, Cardiovascular ultrasound 9 (2011) 35. doi:10.1186/1476-7120-9-35.

[7] A. Elmaraezy, M. E. Morra, A. T. Mohammed, A. Al-Habaa, A. S. Elgebaly, A. A. Ghazy, A. M. Khalil, N. T. Huy, K. Hirayama, Risk of cataract among interventional cardiologists and catheterization lab staff: A systematic review and meta-analysis., Catheterization and cardiovascular interventions : official journal of the Society for Cardiac Angiography & Interventions 90 1 (2017) 1–9.

[8] E. Vano, N. J. Kleiman, A. A. Durán, M. M. Rehani, D. Echeverri, M. Cabrera, Radiation cataract risk in interventional cardiology personnel., Radiation research 174 4 (2010) 490–5.

[9] O. Ciraj-Bjelac, M. M. Rehani, A. Minamoto, K. H. Sim, H. B. Liew, E. Vano, Radiation-induced eye lens changes and risk for cataract in interventional cardiology., Cardiology 123 3 (2012) 168–71.

[10] P. Ortiz-Lopez, L. Dauer, R. Loose, C. Martin, D. Miller, E. Vano, M. Doruff, R. Padovani, G. Massera, C. Yoder, Icrp publication 139: Occupational radiological protection in interventional procedures, Annals of the ICRP 47 (2018) 1–118. doi:10.1177/0146645317750356.

[11] I. Clairand, J.-M. Bordy, J. Daures, J. Debroas, M. Denozière, L. Donadille, M. Ginjaume, C. Itié, C. Koukorava, S. Krim, A. L.

Lebacq, P. Martin, L. Struelens, M. Merce, M. Tosic, F. Vanhavere, Active personal dosemeters in interventional radiology: Tests in laboratory conditions and in hospitals, Radiation protection dosimetry 144 (2010) 453–8. doi:10.1093/rpd/ncq556.

[12] B. Siebert, R. Thomas, Computational Dosimetry, Radiation Protection Dosimetry 70 (1-4) (1997) 371–378. doi:10.1093/oxfordjournals.rpd.a031980.

[13] K. Eckerman, J. Poston, W. Bolch, X. Xu, Stylized computational phantoms developed at ornl and elsewhere (2009) 43–64doi:10.1201/EBK1420059793-c2.

[14] M. Caon, Voxel-based computational models of real human anatomy: A review, Radiation and environmental biophysics 42 (2004) 229–35. doi:10.1007/s00411-003-0221-8.

[15] G. Xu, An exponential growth of computational phantom research in radiation protection, imaging, and radiotherapy: A review of the fifty-year history, Physics in medicine and biology 59 (2014) R233–R302. doi:10.1088/0031-9155/59/18/R233.

[16] A. Badal, A. Badano, Accelerating monte carlo simulations of photon transport in a voxelized geometry using a massively parallel graphics processing unit, Medical physics 36 (2009) 4878–80. doi:10.1118/1.3231824.

[17] A. Badal, F. Zafar, H. Dong, A. Badano, A real-time radiation dose monitoring system for patients and staff during interventional fluoroscopy using a GPU-accelerated Monte Carlo simulator and an automatic 3D localization system based on a depth camera, in: R. M. Nishikawa, B. R. Whiting, C. Hoeschen (Eds.), Medical Imaging 2013: Physics of Medical Imaging, Vol. 8668, International Society for Optics and Photonics, SPIE, 2013, pp. 600 – 610. doi:10.1117/12.2008031.

[18] D. B. Pelowitz, MCNPX TM User's manual version 2.7.0, 2011. doi:LA-CP-05-0369.

[19] J. Shotton, A. Fitzgibbon, M. Cook, T. Sharp, M. Finocchio, R. Moore, A. Kipman, A. Blake, Real-time human pose recognition in parts from

single depth images, Studies in Computational Intelligence 411 (2013) 119–135. arXiv:1111.6189v1, doi:10.1007/978-3-642-28661-2-5.

[20] Q. Wang, G. Kurillo, F. Ofli, R. Bajcsy, Evaluation of pose tracking accuracy in the first and second generations of microsoft kinect, in: International Conference on Healthcare Informatics, 2015, pp. 380–389. doi:10.1109/ICHI.2015.54.

[21] K. Otte, B. Kayser, S. Mansow-Model, J. Verrel, F. Paul, A. U. Brandt, T. Schmitz-Hübsch, Accuracy and reliability of the kinect version 2 for clinical measurement of motor function, PLOS ONE 11 (11) (2016) 1–17. doi:10.1371/journal.pone.0166532.

[22] M. Jebeli, A study on validating kinectv2 in comparison of vicon system as a motion capture system for using in health engineering in industry, Nonlinear Engineering Modeling and Application 6 (2017) pp. 95–99. doi:10.1515/nleng-2016-0017.

[23] P. A. Lombardo, F. Vanhavere, A. L. Lebacq, L. Struelens, R. Bogaerts, Development and Validation of the Realistic Anthropomorphic Flexible (RAF) Phantom, Health Physics 114 (5) (2018) 489–499. doi:10.1097/HP.0000000000000805.

[24] M. Ginjaume, E. Carinou, M. Brodecki, I. Clairand, J. Domienik-Andrzejewska, L. Exner, P. Ferrari, Z. Jovanovic, D. Krstic, S. Principi, O. Van Hoey, F. Vanhavere, Effect of the radiation protective apron on the response of active and passive personal dosemeters used in interventional radiology and cardiology, Journal of Radiological Protection 39. doi:10.1088/1361-6498/aaf2c0.

[25] I. Nuclear Technology Services, Bottle mannequin absorber (bomab) phantom, accessed: 2019-11-13.
URL `https://www.ntsincorg.com/bomab_phantom.htm`

Highlights

- MC simulations can accurately calculate doses in interventional radiology fields
- Motion tracking system based on depth-cameras was developed to be used in cath-labs
- An application was developed to generate MCNP input files from radiation dose reports
- Clinical validation tests showed differences between measurements and simulations

Author declaration

1. Conflict of Interest

Potential conflict of interest exists:

We wish to draw the attention of the Editor to the following facts, which may be considered as potential conflicts of interest, and to significant financial contributions to this work:

The nature of potential conflict of interest is described below:

☒No conflict of interest exists.

We wish to confirm that there are no known conflicts of interest associated with this publication and there has been no significant financial support for this work that could have influenced its outcome.

2. Funding

☒Funding was received for this work.

All of the sources of funding for the work described in this publication are acknowledged below:

This work was part of PODIUM project which is funded by the CONCERT-European Joint Programme for the Integration of Radiation Protection Research 2014-2018" under grant agreement No. 662287.

☐No funding was received for this work.

3. Intellectual Property

☒We confirm that we have given due consideration to the protection of intellectual property associated with this work and that there are no impediments to publication, including the timing of publication, with respect to intellectual property. In so doing we confirm that we have followed the regulations of our institutions concerning intellectual property.

4. Research Ethics

☒We further confirm that any aspect of the work covered in this manuscript that has involved human patients has been conducted with the ethical approval of all relevant bodies and that such approvals are acknowledged within the manuscript.

☐IRB approval was obtained (required for studies and series of 3 or more cases)

☐Written consent to publish potentially identifying information, such as details or the case and photographs, was obtained from the patient(s) or their legal guardian(s).

5. Authorship

The International Committee of Medical Journal Editors (ICMJE) recommends that authorship be based on the following four criteria:

1. Substantial contributions to the conception or design of the work; or the acquisition, analysis, or interpretation of data for the work; AND
2. Drafting the work or revising it critically for important intellectual content; AND
3. Final approval of the version to be published; AND
4. Agreement to be accountable for all aspects of the work in ensuring that questions related to the accuracy or integrity of any part of the work are appropriately investigated and resolved.

All those designated as authors should meet all four criteria for authorship, and all who meet the four criteria should be identified as authors. For more information on authorship, please see http://www.icmje.org/recommendations/browse/roles-and-responsibilities/defining-the-role-of-authors-and-contributors.html#two.

☐All listed authors meet the ICMJE criteria. ☐We attest that all authors contributed significantly to the creation of this manuscript, each having fulfilled criteria as established by the ICMJE.

☐One or more listed authors do(es) not meet the ICMJE criteria.

We believe these individuals should be listed as authors because:

[Please elaborate below] ☐

☒We confirm that the manuscript has been read and approved by all named authors.

☒We confirm that the order of authors listed in the manuscript has been approved by all named authors.

6. Contact with the Editorial Office

The Corresponding Author declared on the title page of the manuscript is:

Mahmoud Abdelrahman

☒This author submitted this manuscript using his/her account in EVISE.

> ☒We understand that this Corresponding Author is the sole contact for the Editorial process (including EVISE and direct communications with the office). He/she is responsible for communicating with the other authors about progress, submissions of revisions and final approval of proofs.
>
> ☒We confirm that the email address shown below is accessible by the Corresponding Author, is the address to which Corresponding Author's EVISE account is linked, and has been configured to accept email from the editorial office of American Journal of Ophthalmology Case Reports:
>
> *mabdelra@sckcen.be*

☐Someone other than the Corresponding Author declared above submitted this manuscript from his/her account in EVISE:

> ☐We understand that this author is the sole contact for the Editorial process (including EVISE and direct communications with the office). He/she is responsible for communicating with the other authors, including the Corresponding Author, about progress, submissions of revisions and final approval of proofs.

We the undersigned agree with all of the above.

Author’s name (Fist, Last)	Signature	Date
1. Pasquale Lombardo		
2. Filip Vanhavere		
3. Alain Seret		
4. Christophe Phillips		
5. Peter Covens		
6.		
7.		
8.		
9.		

Conflict of Interest and Authorship Conformation Form

Please check the following as appropriate:

- ☒ All authors have participated in (a) conception and design, or analysis and interpretation of the data; (b) drafting the article or revising it critically for important intellectual content; and (c) approval of the final version.
- ☒ This manuscript has not been submitted to, nor is under review at, another journal or other publishing venue.
- ☒ The authors have no affiliation with any organization with a direct or indirect financial interest in the subject matter discussed in the manuscript
- ○ The following authors have affiliations with organizations with direct or indirect financial interest in the subject matter discussed in the manuscript:

Author's name	Affiliation